

SEISMIC SOURCES

INTRODUCTION	2
HISTORICAL DEVELOPMENT	2
NEAR AND FAR-FIELD	4
SOURCE PARAMETERS	6
FOCAL TIME	7
LOCATION	8
MAGNITUDE	9
LOCAL MAGNITUDE	9
BODY WAVE MAGNITUDE	9
SURFACE WAVE MAGNITUDE	10
DURATION MAGNITUDE	10
MOMENT MAGNITUDE	10
MACROSEISMIC MAGNITUDE	11
COMPARISON OF MAGNITUDES	11
SEISMIC ENERGY	12
SEISMIC MOMENT	13
MOMENT TENSOR	14
STRESS DROP	16
SOURCE TIME FUNCTION	18
RADIATION PATTERN	19
DIRECTIVITY	20
SOURCE SPECTRUM	21
MODELS	23
REID	23
HASKELL	24
BRUNE	27
COMPARISON OF MODELS	31
SOURCES OF ERRORS	32

Suggested literature:

- Bullen, K.E. & Bolt, B.A. 1985. An introduction to the theory of seismology. 4th edition, Cambridge University Press.
- Gibowicz, S.J. & Kijko, A. 1994. An introduction to mining seismology. Academic Press, Inc., San Diego, California.
- Lay, T. & Wallace, T.C. 1995. Modern global seismology. Academic Press, Inc.
- Scholz, C.H. 1990. The mechanics of earthquakes and faulting. Cambridge University Press.

INTRODUCTION

HISTORICAL DEVELOPMENT

First ideas on the nature of earthquakes were expressed by Thales of Miletas of Greece (625 - 547 BC) who assumed the earth to float on water. Undulations of the water surface were claimed to be the cause of earthquakes. Seneca (4 BC - 65 AC) disagreed with Thales for he concluded, that - if Thales was correct - the earth would tremble all the time, and periods of quietness were more astonishing than continuous earth movements. Anaxagoras of Klazomenai (500 - 428 BC) assumed an ether protruding from the earth body as the cause of tremors. Anaximenes of Miletas (585 - 526 BC) claimed seasonal variations being responsible for quakes: dry and wet seasons cause earthquakes. Later, Demokrit of Abdera (460 - 371 BC) concentrated on wet seasons and suggested rainwater triggering earthquakes. One of the greatest philosophers, Aristotle (384 - 322 BC), assumed the escape of compressed air trapped in the earth's interior as the reason for earthquakes. Plinius (23 - 79 AC), author of the 'historia naturalis', considered earthquakes simply as underground thunder storms. Much later, in the 16th century, Georgius Agricola (1494 - 1555) thought earthquakes as a result of underground fires which are inflamed by the sun. An idea which reflects his knowledge of mining operations, where the principle of setting underground fire was used to mine ore deposits. The idea of underground fires was later pursued by Athanasius Kircher (1601 - 1680), and reappeared every now and then until the turn of the 19th century. In addition, many scientists believed earthquakes to be an expression of ongoing volcanism until 1900.

However, in 1883 Grove K. Gilbert published a short article in the *Salt Lake City Tribune* stating: *'the upthrust¹ produces a local strain in the crust, involving a certain amount of compression and distortion, and this strain increases until it is sufficient to overcome the starting friction along the fractured surface. Suddenly, and almost instantaneously, there is an amount of motion sufficient to relieve the strain, and this is followed by a long period of quiet, during which the strain is gradually reimposed.'*

Gilbert carries on to recognize the intermittent nature of earthquake recurrences: *'The spot which is the focus of an earthquake ... is therefore exempt [from a recurrence] for a long time, and conversely, any locality on the fault line of a large mountain range which has been exempt from earthquakes for a long time, is by so much nearer to the date of recurrence.'*

Concrete concepts of seismic sources appeared only in the early 20th century, when the theory of wave propagation (e.g. Poisson, Rayleigh) was established and seismic instruments (e.g. Milne, Wiechert) became available.

¹ Gilbert is referring to the block-mountain formation in the Great Basin
Lenhardt

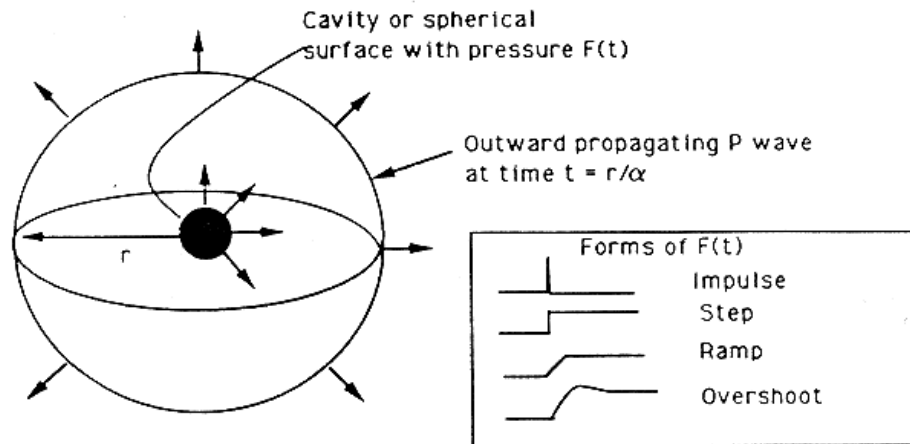
Year	Name	Remarks
1910	Harry Fielding Reid	'Strain rebound concept': strain accumulation near faults - release of the strain = earthquake, based on displacement measurements after the 1906 San Francisco earthquake. Estimated energy release.
1920/24	A.A. Griffith	energy balance of a propagating crack, based on the theorem of minimum energy.
1959	Leon Knopoff & Freeman Gilbert	step source time function
1959	Vladimir I. Keilis-Borok	stress drop from moment and source radius
1964	Norman A. Haskell	'Haskell model', ramp source time function, amplitude spectrum flat at low frequencies
1967	Keiiti Aki	characteristic frequency. Renamed to 'corner frequency' in 1971 by Wyss, Hanks & Liebermann
1970	James N. Brune	'Brune model', smoothed ramp source time function, instantaneous radial slip
1970	Freeman Gilbert	moment tensor, forward modelling
1973	Freeman Gilbert	moment tensor inversion
1977	Shamita Das & Keiiti Aki	barrier-model
1978	James D. Byerlee	'Friction law': shear stress = 0,85 * normal stress for normal stresses < 200 MPa
1978	S. Hartzell, F. Wu	empirical Green functions
1979	Keiiti Aki	asperities and barriers
1981	Adam Dziewonski	centroid moment tensor
1990	Thomas H. Heaton	self-healing phase (actually Madariaga introduced the term 'healing' already in 1976)

Suggested literature:

An Introduction to Seismological Research - History and Development, by Benjamin F. Howell Jr., Cambridge University Press, 1990.

NEAR AND FAR-FIELD

For the purpose of discussing the difference between the near- and the far-field terms of the displacement field, we consider a simple point source (explosion).



lw0801

The equation of motion is given by a one-dimensional wave equation:

$$\frac{\partial^2 \Phi}{\partial r^2} - \frac{1}{v_p^2} \frac{\partial^2 \Phi}{\partial t^2} = -4\pi F(t) \delta(r - r_e)$$

with ' $F(t)$ ' = force function (reduced displacement potential, unit ' m^3 ') applied at the elastic radius ' r_e ', and ' r ' being the distance from the elastic radius, and ' v_p ' = velocity of the compressional wave. The displacement potential (unit ' m^2 ') has then the form

$$\Phi(r, t) = -\frac{F\left(t - r/v_p\right)}{r}$$

The spherical displacement field (unit ' m ') is then given by

$$u(r, t) = \frac{\partial \Phi(r, t)}{\partial r} = \underbrace{\left(\frac{1}{r^2}\right) F\left(t - \frac{r}{v_p}\right)}_{\text{near-field}} + \underbrace{\left(\frac{1}{rv_p}\right) \frac{\partial F\left(t - r/v_p\right)}{\partial \tau}}_{\text{far-field}}$$

with $\tau = t - r/v_p$ as the 'retarded' time. Only after ' τ ' turned positive (at the time of the arrival of the wave), the surrounding medium is affected.

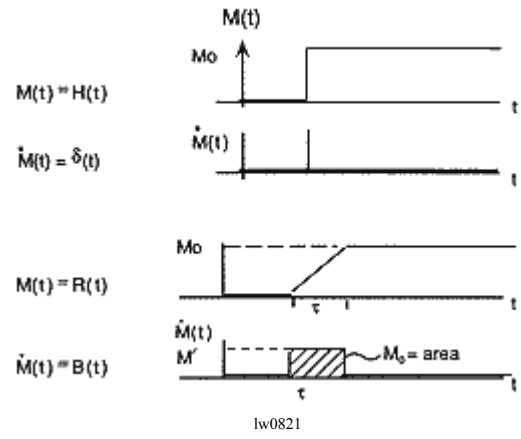
The first term decays with $1/r^2$ and is called the **near-field term**.

The second term decays with $1/r$ and is called the **far-field term**.

The force-term 'F' describes the "strength" of the source, the time history of 'F(t)' is related to the seismic moment via

$$M(t) = -4\pi\rho v_p^2 F(t)$$

Hence, the far-field term of the displacement represents the time derivative of the history of the moment $\dot{M}(t)$.



Far-field P- and S-wave displacement amplitudes are proportional to $\dot{M}(t)$, the time derivative of the seismic moment function $M(t) = GA(t)D(t)$. 'G' = shear modulus, 'A' = area, 'D' = displacement. Simple step and ramp moment functions would generate far-field impulses or boxcar ground motions.

near field	r (distance) $\ll \lambda$ (wavelength)	$u(t) \cong M(t)$
far field	r (distance) $\gg \lambda$ (wavelength)	$u(t) \cong \dot{M}(t)$

SOURCE PARAMETERS

Depending on the resolution of the measurement equipment, different kinds of seismic sources can be distinguished:

	type	example
1.	shear slip	tectonic 'earthquake'
2.	tensile failure	roof collapse in mines, karst
3.	explosion	volcanic, blast, nuclear test
4.	implosions	phase transition in deep subduction events
5.	impact	meteorite, bomb
6.	short duration 'noise'	aeroplanes travelling at super sonic speed
7.	ambient noise	microseisms due to remote weather conditions

All of these sources can be represented by a combination of forces. Many of the failure processes can be modelled in laboratory tests.

The following source parameters are important for describing the source:

1.	focal time
2.	location
3.	magnitude
4.	seismic energy
5.	seismic moment
6.	stress drop
7.	source time function
8.	source spectrum

Note: Moment tensor inversions, rise time, duration of the source pulse and seismic efficiencies add to the knowledge about the source. In case of tectonic earthquakes, the extent of the source, the fault orientation, slip vectors, rupture velocities and spatial stress drops should be considered, too.

FOCAL TIME

Kiyoo Wadati² discovered deep focus earthquakes near Japan by using arrival times of seismic waves at several stations. The method is also useful when estimating the focal time 't₀' of shallow seismic sources, and is based on a diagram in which P-arrivals 't_p' are plotted against the time difference between S- and P-arrivals 't_s-t_p' of several stations.

$$t_p = \frac{\Delta}{v_p} + t_0$$

$$t_s - t_p = \frac{\Delta}{v_s} - \frac{\Delta}{v_p}$$

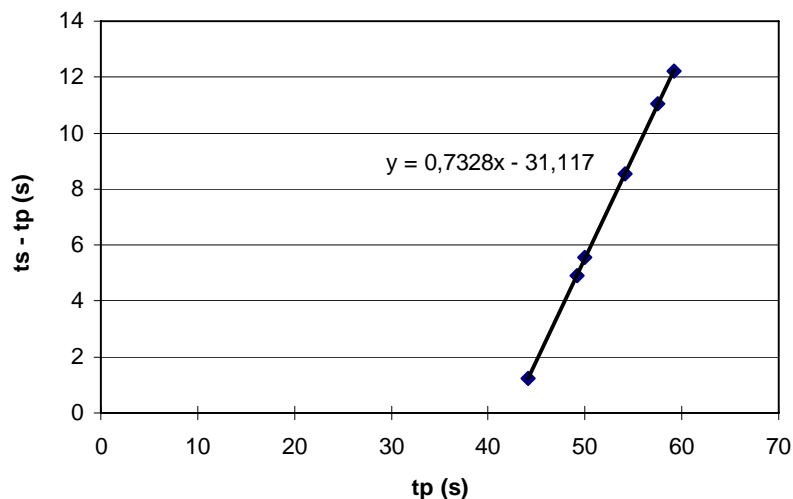
$$t_s - t_p = \Delta \left(\frac{1}{v_s} - \frac{1}{v_p} \right)$$

$$t_s - t_p = \frac{\Delta}{v_p} \left(\frac{v_p}{v_s} - 1 \right)$$

$$t_s - t_p = (t_p - t_0) \left(\frac{v_p}{v_s} - 1 \right)$$

Example:

distance Δ (km)	t _p (s)	t _s -t _p (s)
10	44,17	1,23
40	49,17	4,95
45	50,00	5,56
70	54,17	8,63
90	57,50	11,10
100	59,17	12,24



The focal time 't₀' is finally given by e.g.

$$t_0 = t_p - \left(\frac{\Delta}{v_p} \right)$$

Hence, spatial changes of velocities (strong gradients, caustics) may have an effect on the correct determination of the focal time. Note, that there are other methods to determine the focal time, too. Locating earthquakes usually involves also determining the focal time as a by-product. Errors in phase pickings are mainly compensated in a wrong depth and an erratic focal time during the location procedure.

² Wadati, K. 1933. On traveltimes of earthquake waves. Part II, Geoph.Mag.7, Tokyo, Japan.
Lenhardt

LOCATION

General: Best solution is given by the global minimum of residuals.

Geiger-Method (1912)

Classic approach. Sum of squared time-residuals \mathbf{r} ('misfit function') has to become a minimum.

Bayesian Approach

Location algorithm is extremely efficient. Assumption: Time residuals are Gaussian distributed. Hypocentre must be close to mine workings.

Location with Approximate Velocity Models

Generalization of the Least-Square Procedure. Assumption: Velocity model consists of random variables. Their deviations from an average model are Gaussian distributed.

Relative Location Technique (ATD = arrival time difference)

All P-wave-arrivals of particular event are related to a reference event. The difference of arrival-times is minimized by adjusting the coordinates and focal time of the master event.

Simultaneous Hypocenter and Velocity Determination

Simultaneous location of a group of seismic events and the velocity model. Follows ATD-technique. Known as *Simultaneous structure and hypocenter* (SSH) determination or *Joint determination of hypocentres* (JHD). The method does not require calibration blasts, is fast and can be run on small computers.

Other Location Methods

Linear Methods

Fast and free from iterative problems. Requires constant velocity-model.

Large Time Residuals and L1 Norm

Takes account of arrival time-residuals, which are not Gaussian distributed.

Nelder-Mead Simplex Procedure

Relatively slow, but avoids calculation of derivatives (which can be very small, thus leading to ill-conditioned matrices).

MAGNITUDE

LOCAL MAGNITUDE

Several magnitude scales are in use. The first ‘scale’ was introduced by Charles Francis Richter³ in the early 1930s. He compared amplitudes of ground displacements which were recorded with a Wood-Anderson torsion seismometer (free period 0,8”, high frequency magnification 2800). He calculated the ‘size’ or ‘strength’ of a seismic event by relating it to a ‘master event’ at a distance of 100 km which appeared on a Wood-Anderson seismograph with an amplitude of 1 mm. Such an event was addressed as an earthquake having a local magnitude of ‘0’. Local magnitudes are also referred to as ‘Richter’-magnitudes. The original relation is:

$$m_l = \log(A) - \log(A_0)$$

with ‘A₀’-values being tabulated for several distances in Richter (1958)⁴ to ease calculations. Taking into account the involved reference distance of 100 km, one may also rewrite the above equation as

$$m_l = \log(A) - 2.48 + 2.76\log(\Delta)$$

This formula is still applicable when considering a Wood-Anderson seismometer response. Other forms of this formula involve other constants to cater for different crustal models, instruments, kinds of input signals, etc. Local magnitudes are derived from shear wave amplitudes having a period below 1 second which is very useful because buildings exhibit similar periods.

BODY WAVE MAGNITUDE

At larger distances short period measurements become more and more meaningless. Therefore, amplitudes recorded from direct P-waves are used to determine the so-called body wave magnitude:

$$m_b = \log(A/T) + Q(h, \Delta)$$

with ‘A’ being the actual ground-motion amplitude in micrometers, and ‘T’ being the period in seconds. ‘Q’ represents a correction term for focal depth ‘h’ (km) and distance ‘Δ’ (°). ‘Q’ ranges between 0 and 4.25. The magnitude is usually determined from signals having a period around 1 second. These magnitudes tend to scatter a lot, usually in the order of +/-0,3 for individual stations. If very long-period waves – say 5 – 15 seconds – are used, the magnitude is then referred to as ‘m_B’.

³ Richter, C.F. 1935. An instrumental earthquake magnitude scale. Bull.Seism.Soc.Am., Vol.25, 1-32.

⁴ Richter, C.F. 1958. Elementary Seismology. Freeman & Company, San Francisco, 768 pp.

SURFACE WAVE MAGNITUDE

At much larger distances (> 600 km) long-period seismometers are used for magnitude determinations of shallow earthquakes.

$$M_s = \log(A_{20}) + 1.66 \log(\Delta) + k$$

'A₂₀' represents the amplitude in micrometers at a period of 20 seconds, and 'k' is a constant (= 2.0, if the period is 20 seconds, and the distance is given in degrees). In Austria we use $M_s = \log(V) + 1.66 \log(\Delta) + 0.52 - \log(T)$, with V = half peak2peak amplitude in nm/s, Δ = distance in degrees, T = period in seconds.

DURATION MAGNITUDE

Another way to establish the 'size' on an earthquake from the duration of the recorded earthquake. Usually used, when amplitudes cannot be ascertained. Often, the duration 'T_D' is defined between 5% above noise and the time when the signal resumes the same level. The magnitude is then estimated by using e.g.

$$M_D = \log(T_D) + k_1 \log(\Delta) + k_2$$

with 'k₁' and 'k₂' as local constants.

MOMENT MAGNITUDE

The moment magnitude was introduced by Hanks & Kanamori (1979)⁵. This magnitude is independent of the frequency of the signal. The magnitude is denoted as 'M_w' and implies a constant stress drop of 10⁻⁴ of the shear modulus, which is reasonable for tectonic earthquakes:

$$M_w = \frac{2}{3} \log(M_0) - 6.1$$

where 'M₀' represents the seismic moment (Nm). The latter is determined from the spectrum of ground displacement.

Why constant stress drop?

$$E_s = \frac{1}{2} \Delta \sigma D A \quad \text{and} \quad M_0 = G A D \quad \text{than} \quad E_s = \frac{\Delta \sigma}{2G} M_0,$$

hence, if $\log(E_s) = 4.8 + 1.5M$ with E_s in Joule, than

$$M = \frac{2}{3} \log(E_s) - \frac{2}{3} 4.8 = \frac{2}{3} \log\left(\frac{\Delta \sigma}{2G} M_0\right) - 3.2 = \frac{2}{3} \log(M_0) + \frac{2}{3} \log\left(\frac{\Delta \sigma}{2G}\right) - 3.2$$

Hence, if $\frac{\Delta \sigma}{G} = 10^{-4} \Rightarrow M_w = \frac{2}{3} \log(M_0) - 6.1$

Note: D = displacement, G = shear modulus, A = area, Δσ = shear stress drop

⁵ Hanks, T.C. & Kanamori, H. 1979. A moment-magnitude scale. J.Geoph.Res. 84, 2348-2350.

MACROSEISMIC MAGNITUDE

The macroseismic magnitude was used mainly in Europe after the introduction of the magnitude by Richter in California. The macroseismic magnitude is based on epicentral intensities. After the focal depth had been established from the decay of intensities with distance, the epicentral intensity ‘ I_0 ’ and the focal depth are used to estimate a magnitude. A common relation is (Shebalin, 1958)⁶:

$$M_m = \frac{2}{3}I_0 + \frac{7}{3}\log(z) - 2$$

The focal depth can be estimated from the decay of intensities according to (Sponheuer, 1960)⁷

$$I_{local} = I_0 - 3\log\left(\frac{R}{z}\right) - 1.3\alpha(R - z)$$

with ‘ α ’ being the coefficient of absorption which usually varies between 0.001 and 0.01. In Austria ‘ α ’ amounts to 0.002, but varies a lot.

COMPARISON OF MAGNITUDES

Type of magnitude	Applicable frequency	Range
Local magnitude m_l	> 1 Hz	<5
Body wave magnitude m_b	1 Hz	<6
Surface wave magnitude M_S	0.05 Hz	<8
Duration magnitude M_D	-	-
Moment magnitude M_w	Unlimited	Unlimited
Macroseismic magnitude M_m	-	-

Note:

1. m_l is often hampered by local inhomogeneities and radiation pattern effects
2. m_b is quicker to determine but less accurate
3. M_S is often only a rough estimate because signals with a period of 20 seconds are not standard
4. M_D is the least accurate magnitude
5. The use of first capitals is not consistent. Hence, one may find ‘ m_b ’ and ‘ M_b ’, and the like
6. There are other magnitudes in use, too – such as the ‘Nuttli’-magnitude in Canada, or the energy-magnitude by Berckhemer & Purcaru

Within applicable frequency bands the magnitudes should not differ much. Problems may occur with recordings of limited bandwidth.

⁶Shebalin, N. 1958. Correlation between earthquake magnitude and intensity. *Studia geophys. et geod.* 2, 86-87.

⁷Sponheuer, W. 1960. Methoden zur Herdtiefenbestimmung in der Makroseismik. Freiburger Forschungsheft C88, Akademie-Verlag Berlin.

SEISMIC ENERGY

Only a fraction of the total strain energy 'E_T' released during an earthquake is emitted as seismic energy 'E_S'. The other part of the energy is released as heat 'E_H' or is absorbed by non-elastic processes. The strain energy released by a crack of length 'L' is

$$E_T = E_S + E_H = \gamma\pi GD^2 L = \bar{\sigma}DA$$

with 'γ' as constant depending on the fault geometry and stress drop, 'D' is the maximum fault slip, and 'σ̄' = average shear stress (before and after the earthquake) (Starr, 1928 in Bullen & Bolt, 1985⁸)

The seismic energy is given by $E_S = E_T - E_H = E_T \left(1 - \frac{E_H}{E_T}\right) = E_T \eta$

with 'η' as 'seismic efficiency', which theoretically may vary between '0' (= mainly heat is emitted by the source, or non-elastic processes dominate) and '1' (all strain energy is converted into seismic energy), but ranges mostly between 0.1 and 0.01, thus depending strongly on the kind of the source.

The seismic energy itself can be estimated from seismic recordings by using the decrease in energy per unit area on the wave front, normally referred to as 'geometrical spreading'. The energy at a particular station at distance 'Δ' (in degrees) is given by

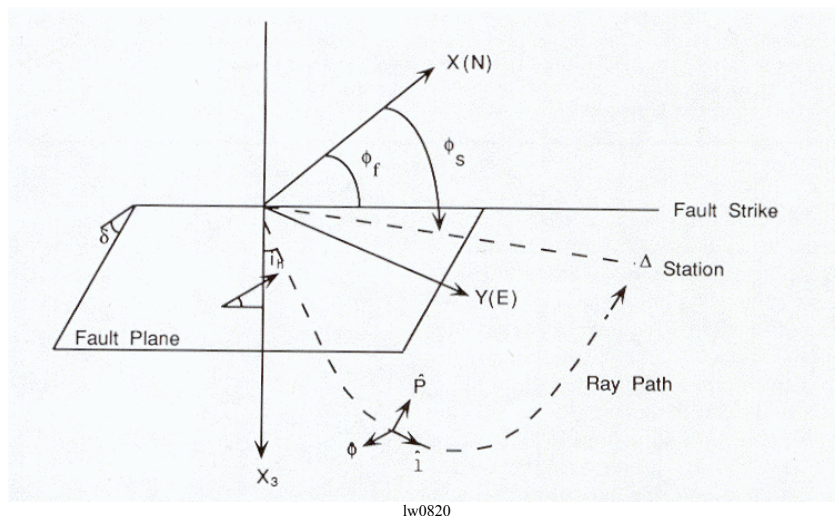
$$E_S(\Delta) = \frac{E_S \sin i_h v_S}{\cos i_0 r_0^3 \sin \Delta \cos i_0} \left| \frac{\partial^2 T}{\partial \Delta^2} \right|$$

$$E_S(\Delta) = \frac{E_S \sin i_h}{r_0 \sin \Delta \cos i_0} \left| \frac{\partial i_h}{\partial \Delta} \right| \Rightarrow E_S = \frac{E_S(\Delta) r_0 \sin \Delta \cos i_0}{\sin i_h \left| \frac{\partial i_h}{\partial \Delta} \right|}$$

$$\Downarrow$$

$$E_S(\Delta) = \rho v_S \omega^2 |u(\omega)|^2$$

with 'r₀' = radius of the earth, 'i_h' = take off angle at the source, 'i₀' = angle of incidence at receiver, 'ρ' = density, 'v_S' = shear wave velocity at point of observation, '|u(ω)|²' = power spectrum of ground displacement at station. In this case, source related radiation effects and absorption are ignored. The formulae still yields useful estimates of seismic energies.



lw0820

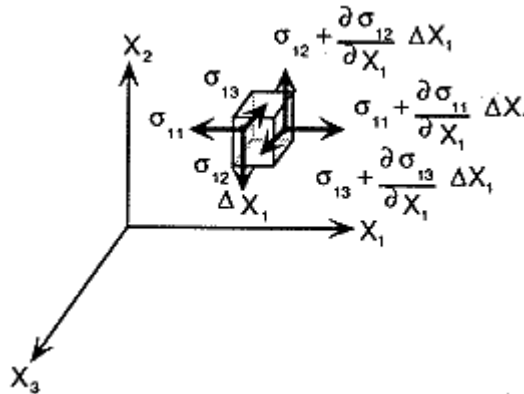
⁸ Bullen & Bolt, 1985. An Introduction to the Theory of Seismology. Cambridge University Press, p.403.

SEISMIC MOMENT

A moment of a force system is the vector product of the force with the position vector of the point of application. Two parallel forces form a couple with a definite moment.

In 1958 Steketee proved the **fundamental equivalence theorem**: *A displacement field produced by the dislocation 'Δu' on a plane element 'δS' in an elastic body equals that produced by a double couple applied at 'δS'.*

Considering a shear dislocation 'Δu₁' (in x₁-direction) at the element 'δS' (perpendicular to x₂-axis) of length '2c' (x₁-axis) and thickness '2ε' (x₂-axis), the moment per unit length in x₃-direction due to the forces (actually accelerations) in x₂-direction are given by the integration over 'ε' and 'c'.⁹



lw0206

$$\int_{-\varepsilon}^{\varepsilon} \int_{-c}^c x_1 \rho f_2 dx_1 dx_2 = - \int_{-\varepsilon}^{\varepsilon} \int_{-c}^c x_1 \frac{\partial \sigma_{12}}{\partial x_1} dx_1 dx_2$$

$$= \int_{-\varepsilon}^{\varepsilon} \int_{-c}^c G \frac{\partial u_1}{\partial x_2} dx_1 dx_2$$

(by integration of parts)

$$= G \int_{-c}^c \Delta u_1 dx_1$$

Integration over the whole plane (x₃-axis) leads finally to the scalar moment (let ε → 0, δS → 0)

$$M_O = GAD$$

with 'G' being the shear modulus, 'A' the fault surface and 'D' the average displacement.

The moment can be estimated from the spectral displacement amplitude 'Ω₀' of recorded seismic waves below the corner frequency from (R = distance, v_s = shear wave velocity) at a specific station

$$M_O = 4\pi\rho v_s^3 R \Omega_0$$

and the complete moment tensor is reconstructed from numerous observations at different azimuths and distance ranges giving an idea of the source mechanism (type, orientation, 'strength' = M₀).

⁹ See Bullen, K.E. & B.A. Bolt 1985, p. 424.

MOMENT TENSOR

In 1970 Gilbert introduced the moment tensor for the first time to calculate the displacement at the free surface. The latter is given by the product of moment tensor elements times the corresponding Green's function. The elastodynamic Green's function is a tensor describing the impulse response - a displacement field (tensor) - due to a unit impulse (Dirac pulse) of the medium between source and receiver. Green's functions differ spatially due the inhomogeneity of the Earth.

Moment tensors can be determined from

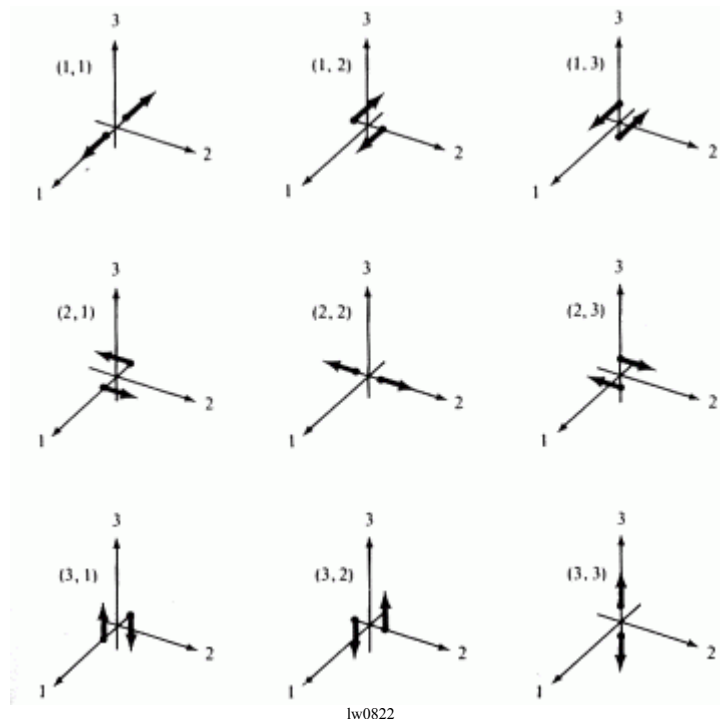
1. free oscillations of the earth
2. long-period surface waves
3. long-period body waves

The moment tensor is a general concept, describing a variety of seismic source models.¹⁰

The moment tensor is given by

$$M_{kj} = \begin{bmatrix} M_{11} & M_{12} & M_{13} \\ M_{21} & M_{22} & M_{23} \\ M_{31} & M_{32} & M_{33} \end{bmatrix} = GA(D_k v_j + D_j v_k)$$

with 'D_i' = slip vector, and 'v_i' = direction of fault normal.



¹⁰ Jost, M.L. & Herrmann, R.B. 1989. A student's guide to and review of moment tensors. Seismological Research Letters, Vol. 60, No.2, 37-57.

Characteristics of the moment tensor:

1. The symmetric moment tensor 'M_{ij}' depends on the seismic source orientation (e.g. fault) and strength.
2. The three diagonal elements represent vector dipoles. The six off-diagonal elements represent force couples.
3. The sum of the eigenvalues denotes the volume change in the source, the 'isotropic part' ('IP').
4. A positive sum indicates an 'explosion' (e.g. nuclear test), a negative sum an 'implosion' (e.g. due to phase transitions).
5. If one eigenvalue vanishes, the deviatoric moment tensor represents a pure 'double couple' ('DC').
6. If none of the eigenvalue vanishes and their sum is still zero, the tensor can be decomposed into a major and a minor double couple – or into a double couple and a compensated linear vector dipole ('CLVD'). The latter is a dipole that is corrected for the effect of volume change (e.g. pillar failure in an underground mine).

The moment tensor can be decomposed in several ways:

1. IP + 3 vector dipoles (= asymmetric change in volume)
2. IP + 3 DC
3. IP + 3 CLVD
4. IP + major DC + minor DC
5. IP + DC + CLVD

In particular, the last option is frequently used to study the nature of seismic sources. It allows to separate the moment tensor into an **isotropic part** (IP), a **double couple** (DC) and a **compensated linear vector dipole** (CLVD).

For the deviatoric eigenvalues $M_1 \geq M_2 \geq M_3$ we compute $\varepsilon = -M_2 / M_3$, and then we get

$$\begin{aligned}
 & \begin{bmatrix} M_1 & 0 & 0 \\ 0 & M_2 & 0 \\ 0 & 0 & M_3 \end{bmatrix} = \\
 & \frac{1}{3} \begin{bmatrix} \text{tr}(\mathbf{M}) & 0 & 0 \\ 0 & \text{tr}(\mathbf{M}) & 0 \\ 0 & 0 & \text{tr}(\mathbf{M}) \end{bmatrix} \quad \text{Isotropic part (IP)} \\
 & + (1 - 2\varepsilon) \begin{bmatrix} 0 & 0 & 0 \\ 0 & -M_3 & 0 \\ 0 & 0 & M_3 \end{bmatrix} \quad \text{Double Couple (DC)} \\
 & + \varepsilon \begin{bmatrix} -M_3 & 0 & 0 \\ 0 & -M_3 & 0 \\ 0 & 0 & 2M_3 \end{bmatrix} \quad \text{Compensated Linear Vector Dipol (CLVD)}
 \end{aligned}$$

with $\text{tr}(\mathbf{M})$ being the trace of the diagonalized moment tensor ' \mathbf{M} ', and ' ε ' is a measure of the size of the 'CLVD' component when compared with the 'DC' and the isotropic part 'IP'.

Note: ' ε ' = 0 for a pure double couple (DC), and 0.5 for a pure CLVD.

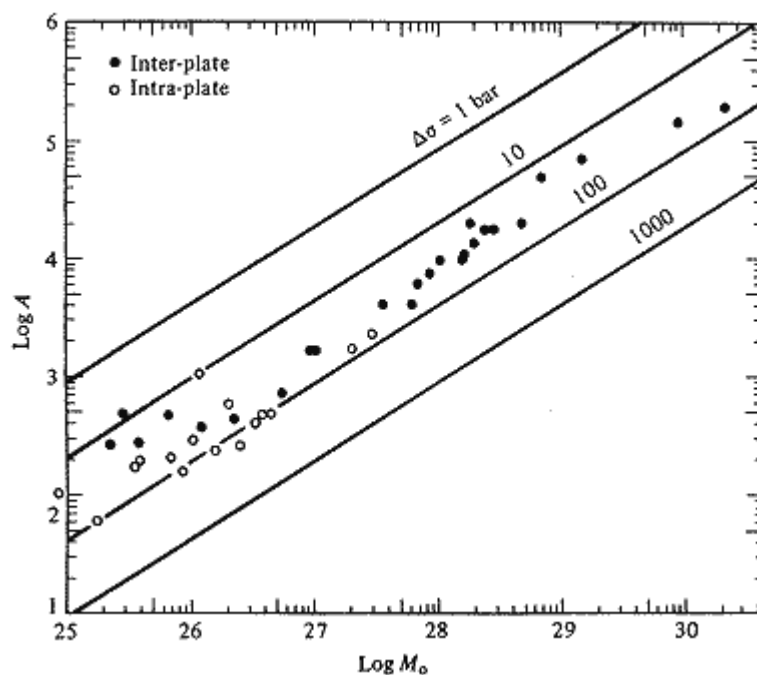
STRESS DROP

Changes of the stress tensor in the earth crust may lead to earthquakes. Only a portion of these stresses are released during earthquakes, however. These stresses can be a result of

1. stress build up due to tectonic forces
2. uplifts
3. changes of the orientation of principal stresses
4. pore water pressure changes
5. impacts
6. intrusions

Definition of the stress drop:

Difference in stress between initial shear stress σ_1 and final shear stress σ_2 ¹¹.



lv0925

'A' = estimated area of fault surface in km². 'M₀' = seismic moment in dyne-cm (subtract 7 from log(M₀) to convert to 'Nm').

Usually, stress drops do not vary much and show only little scatter. Inter-plate earthquakes – along subduction zones – cluster around 3 MPa (30 bars), whereas intra-plate events – collisions inside of plates – tend to slightly higher stress drops of 10 MPa (100 bars).

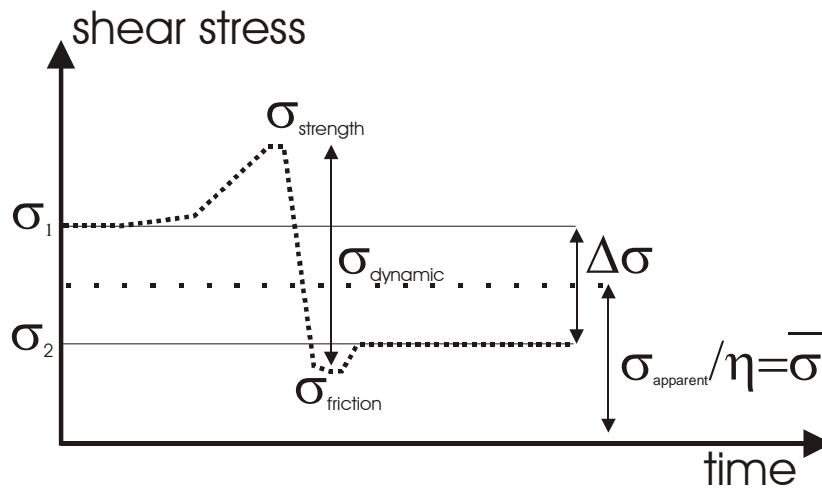
(Figure modified from Kanamori & Anderson, 1975, in Lay & Wallace, 1995)

Suggested literature:

- Brune, J. 1970, 1971. Tectonic stress and the spectra of seismic shear waves from earthquakes. *J.Geophys.Res.* 75, 1970, 4997-5009 (correction in *J.Geophys.Res.* 76, 1971, 5002).
- Boatwright, 1980. A spectral theory for circular seismic sources: Simple estimates of source dimension, dynamic stress drop, and radiated seismic energy. *Bull.Seism.Soc.Am.*, Vol.70, 1-27.
- Hanks, T.C. & McGuire, R. 1981. The character of high frequency strong ground motion. *Bull.Seism.Soc.Am.*, Vol.71, 2071-2096.
- Wyss, M. & Brune, J., 1968. Seismic moment, stress and source dimensions for earthquakes in the California-Nevada region. *J.Geophys.Res.*, Vol.73, 24-42.

¹¹ Note, that σ_1 and σ_2 refer here to shear stresses, and not to principal stresses like in a geomechanics....

We distinguish the following stress drops:



type	author	formulae	comment
Brune (<i>'static'</i>)	Brune (1970, 1971)	$\Delta\sigma = \sigma_B = 2.34 \frac{v_s}{2\pi f_{cS}} = \frac{7}{16} \frac{M_0}{r_0^3}$	Assumes complete excess shear stress release, approximation of 'static stress drop', f_{cS} = corner frequency of shear wave,
partial	Brune et al. (1986)	-	'incomplete' Brune-stress drop
dynamic (<i>effective</i>)	Boatwright (1980)	$\sigma_d = \frac{\sqrt{\rho\rho_0} v_s v_{s0}^{5/2}}{v_r^3} \frac{r}{R_s} (1 - \xi^2)^2 \left \frac{\dot{u}}{t} \right $	calculated from S-wave slope \dot{u}/t , indices '0' refer to the source, $\xi = v_r \sin \theta / v_{s0}$, R_s = radiation pattern of S-wave
dynamic (<i>effective</i>)	Hanks & McGuire (1981)	$\sigma_{rms} = \frac{2.7\rho_0 r}{0.85} \sqrt{\frac{f_{cS}}{f_{max}}} a_{rms}^S$	a_{rms}^S = rms acceleration averaged over duration of S-wave, f_{cS} = corner frequency of shear wave, f_{max} = high frequency limit of recorded S-wave

The **apparent** stress (Wyss & Brune, 1968) is proportional to the dynamic stress drop, but does not represent an actual stress drop, for

$$\sigma_a = \frac{GE_s}{M_0} = \eta \bar{\sigma} = \eta \frac{\sigma_1 + \sigma_2}{2} = \eta \frac{2\sigma_1 + \Delta\sigma}{2}$$

Note, that each earthquake alters the orientation of principal stresses along the fault due to the reduction of shear stresses along the fault plane during the earthquake.

SOURCE TIME FUNCTION

The source time function 's(t)' is needed for waveform modelling and moment tensor inversions. Therefore, the function is found in the complete description of the far-field displacement time series u(t)

$$u(t) = s(t) * g(t) * i(t)$$

with s(t) as the source time function, g(t) is the propagation filter, and i(t) is the transfer function of both, the seismometer and the data acquisition system.

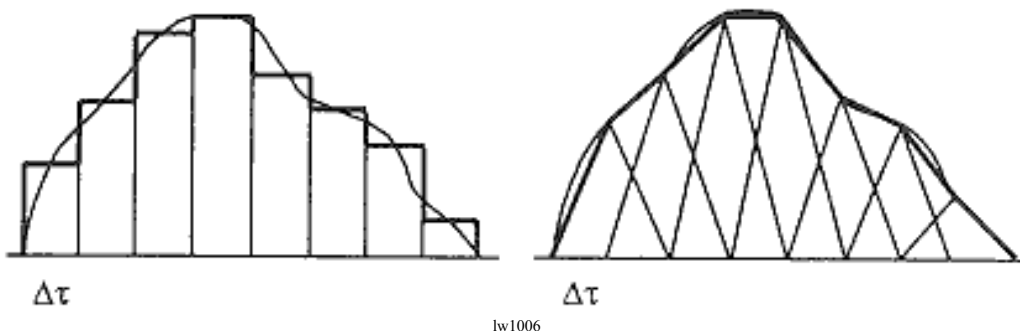
Generally, the *source time function* is defined as

$$s(t) = \sum_{j=1}^N B_j b(t - \tau_j)$$

$$u_n = i(t) * \sum_{j=1}^N \sum_{i=1}^5 B_j m_i [b(t - \tau_j) * G_{in}(t)]$$

with $b(t - \tau_j)$ = length of the boxcar of width $\Delta\tau$, and B_j being the height of each element of $\Delta\tau$ and m_i represents the elements of the moment tensor. The duration of the source time function is given by $N\Delta\tau$.

There are two alternatives for parameterizing arbitrarily shaped source functions (rectangle and triangle):



RADIATION PATTERN

The far-field radiation pattern alters the amplitude (displacement) of recorded signal in radial and two tangential directions as seen from the source¹².

The displacement vector is given by

$$\begin{aligned}
 u_r &= \frac{M}{4\pi Gr^2} \left(1 + \frac{\Gamma}{2}\right) (\sin^2 \theta \sin 2\phi) \\
 u_\theta &= \frac{M}{4\pi Gr^2} \left(\frac{1}{2} - \frac{\Gamma}{2}\right) (\sin 2\theta \sin 2\phi) \\
 u_\phi &= \frac{M}{4\pi Gr^2} (1 - \Gamma) (\sin \theta \cos 2\phi)
 \end{aligned}$$

with

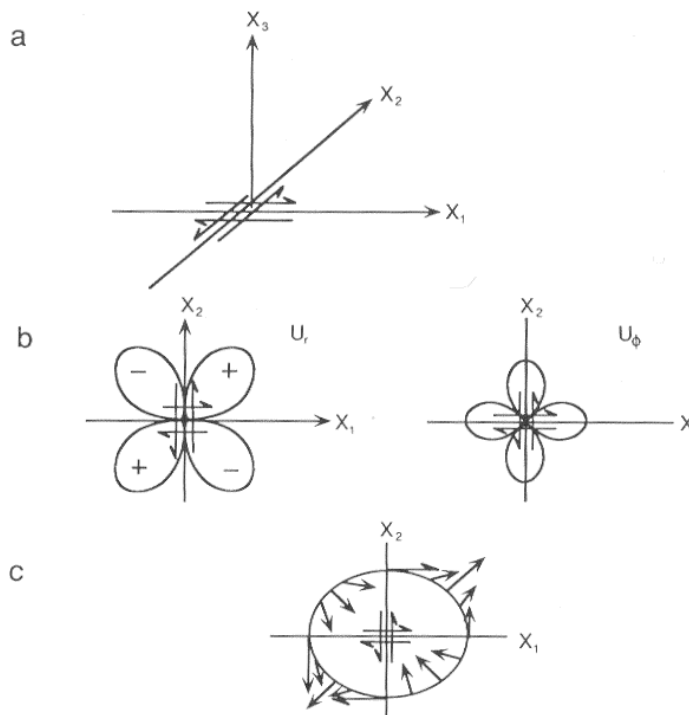
$$\begin{bmatrix} u_r \\ u_\theta \\ u_\phi \end{bmatrix} = \begin{bmatrix} \sin \theta \cos \phi & \sin \theta \sin \phi & \cos \phi \\ \cos \theta \cos \phi & \cos \theta \sin \phi & -\sin \phi \\ -\sin \phi & \cos \phi & 0 \end{bmatrix} \begin{bmatrix} u_1 \\ u_2 \\ u_3 \end{bmatrix}$$

$$\Gamma = \frac{\lambda + G}{\lambda + 2G}$$

and with 'λ' and 'G' being Lamé's constants (if λ = G then Γ = 2/3).

The example below shows the pattern of a double couple in the x₁x₂-plane, where the above formulae (θ = angle from +x₃ = π/2, φ = azimuth measured from +x₂) reduces to

$$\begin{aligned}
 u_r &= \frac{M}{4\pi Gr^2} \left(1 + \frac{\Gamma}{2}\right) \sin 2\phi \\
 u_\phi &= \frac{M}{4\pi Gr^2} (1 - \Gamma) \cos 2\phi \\
 u_\theta &= 0
 \end{aligned}$$



The concept:

The **displacement field due to a shear dislocation** equals the displacement field due to a **distribution of equivalent double couples** that are placed in a medium **without any dislocation**.

Note: The first onset direction of P-wave arrivals can be utilized to determine the orientation of the involved fault plane together with the sense of movement.

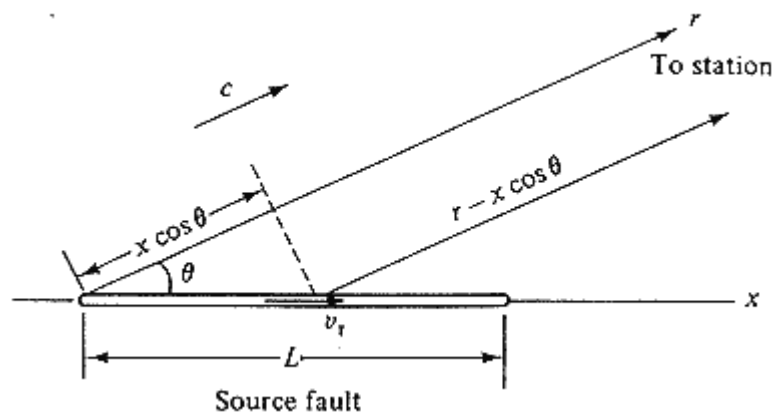
¹² Definition of the coordinate system: +x₁ points East, +x₂ points North and +x₃ points upwards.

DIRECTIVITY

Seismic records reflect the position of a seismic station relative to the seismic source due to

1. radiation pattern
2. the fault length
3. rupture velocity

Since the rupture velocity is smaller than the propagation velocity of shear waves, body waves generated by movement of an additional segment of a fault will arrive earlier than body waves, which are generated later during the rupturing process. The time difference of subsequent arrivals of waves depends on the azimuth between source and receiver.



lw0908

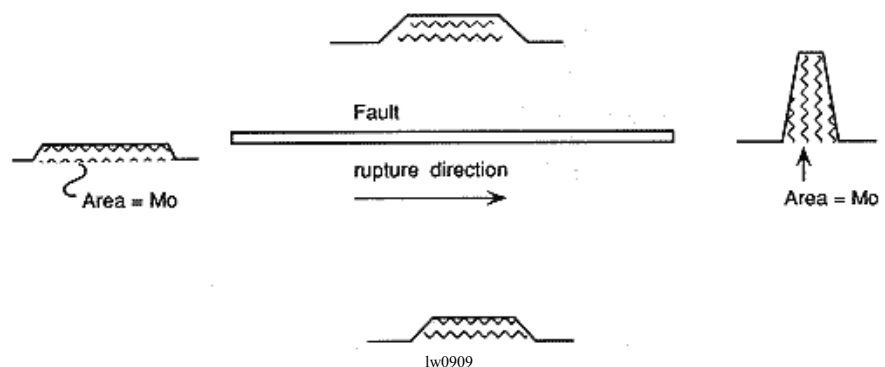
The travel time of a body wave with velocity 'c' from the origin at the fault and a station is

$$t_x = \frac{x}{v_r} + \frac{(r - x \cos \theta)}{c}$$

The arrival time difference ' τ_c ' from waves originating from the beginning and from the end of the fault (apparent rupture duration) define the shape of the recorded ground motion.

$$\tau_c = \left[\frac{L}{v_r} + \frac{(r - L \cos \theta)}{c} \right] - \left(\frac{r}{c} \right) = \frac{L}{v_r} - \frac{L \cos \theta}{c}$$

Azimuthal variability of signals (apparent source time functions) for a rupturing fault as observed in the far-field. The rupture duration and the amplitude changes, depending on the azimuth. The seismic moment, which is represented by the time-integral of the source time function ('Area'), does not change, however.



SOURCE SPECTRUM

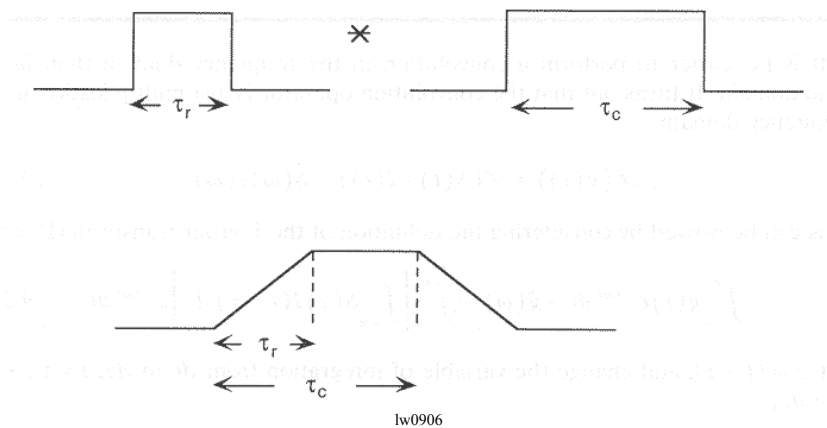
The source time function for faulting mechanisms can be represented as a convolution of the

- particle dislocation history (**rise time**) ‘ τ_r ’ (the time it takes for a particle to achieve its final displacement), and the
- the duration of the faulting process (**rupture duration**) ‘ τ_c ’

Both time histories can be modelled in the far-field by boxcar functions ‘B’. Hence, the far-field ground displacement ‘u(t)’ is given by the convolution of both boxcar functions:

$$u(t) \approx B(t; \tau_r) * B(t; \tau_c)$$

with ‘ M_0 ’ = scalar seismic moment.



Since the Fourier transform of a boxcar functions is given by

$$F(B(t; \tau)) = \frac{\sin(\omega\tau/2)}{\omega\tau/2}$$

the convolution of two boxcar functions leads due to the multiplication in the frequency domain to displacement spectrum

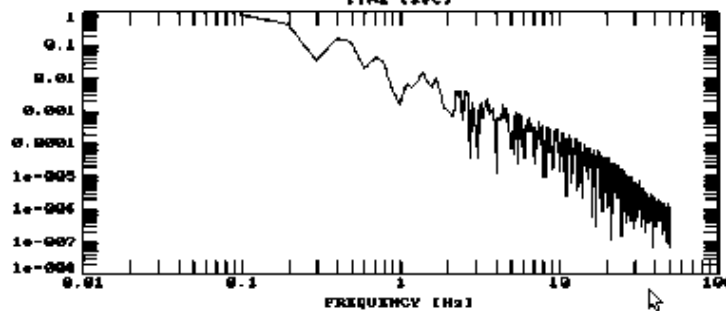
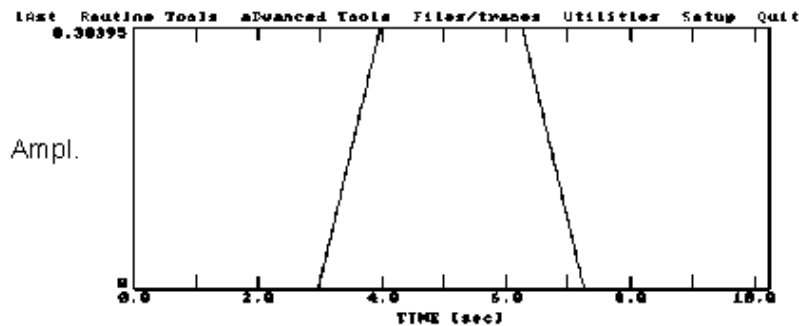
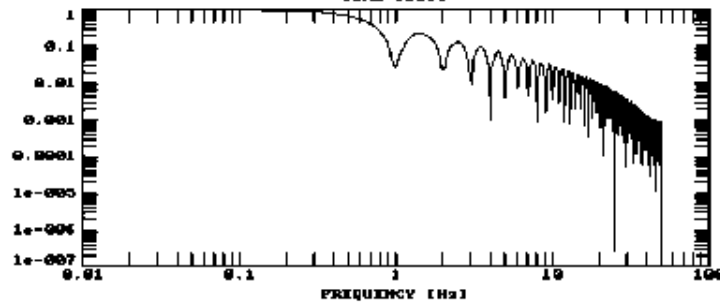
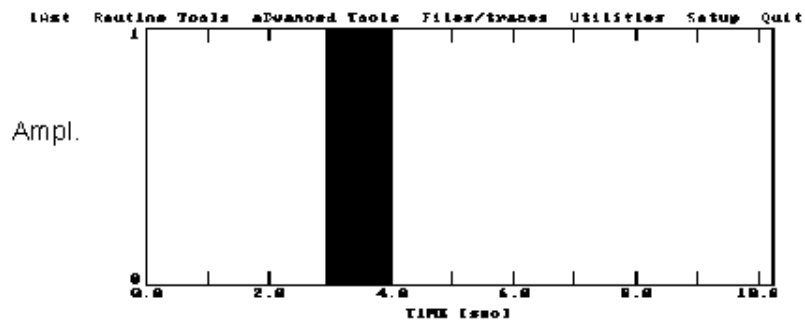
$$u(\omega) \approx \left| \frac{\sin(\omega\tau_r/2)}{\omega\tau_r/2} \right| \left| \frac{\sin(\omega\tau_c/2)}{\omega\tau_c/2} \right|$$

The plateau of that spectrum is defined by amplitudes at frequencies less than $2/\tau_r$. The spectrum then decays according to $1/\omega$. The crossover frequency between the plateau and the $1/\omega^2$ decay is called the

‘corner frequency’.

Hence, if a corrected spectrum (absorption!) just decays with ‘ $1/\omega$ ’, the ground displacement in the far-field can be represented by a single boxcar function. This would mean, that either the rise time or the rupture duration is zero. Hence, either the particle velocity or the rupture velocity must be infinite – or the recording instrument did not cover the needed frequency range up to very high frequencies, where the ‘ $1/\omega^2$ ’ decay in the amplitude spectrum could have been observed.

$$u(\omega) \approx \begin{cases} \Omega_0 & \Rightarrow \quad \omega < \frac{2}{\tau_c} \Rightarrow \text{plateau} \\ \frac{\Omega_0}{\omega\tau_c/2} & \Rightarrow \frac{2}{\tau_c} < \omega < \frac{2}{\tau_r} \Rightarrow \text{crossover, } \omega \text{ decay} \\ \frac{\Omega_0}{\omega^2(\tau_c\tau_r/4)} & \Rightarrow \quad \omega > \frac{2}{\tau_r} \Rightarrow \omega^2 \text{ decay} \end{cases}$$

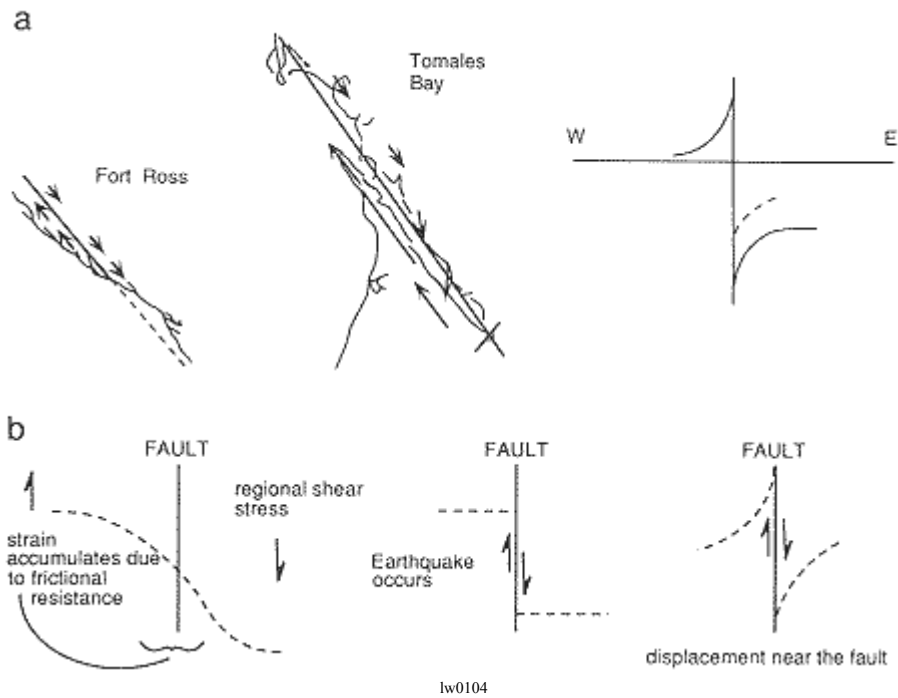


Spectra of a single boxcar (a) and of a trapezoid (= two convolved boxcars).

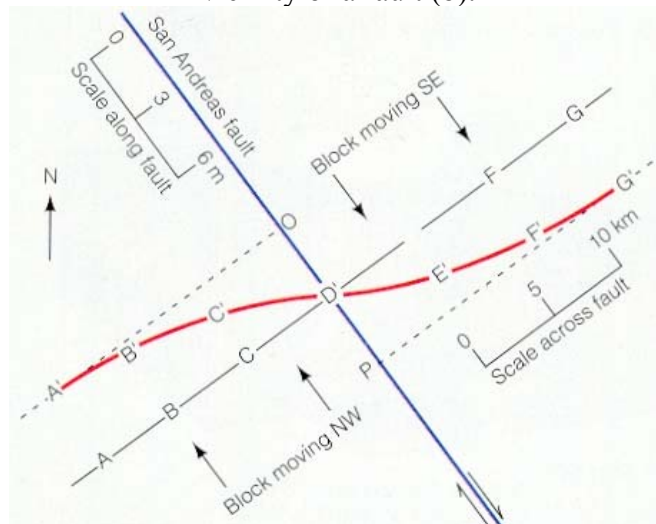
MODELS

REID

The horizontal deformation in the vicinity of the San Andreas fault due to the disastrous San Francisco earthquake in 1906 exhibited a simple symmetry that led Harry Fielding Reid¹³ to formulate the **elastic rebound theory** of earthquakes. The theory states, that strain accumulates prior to an earthquake. The actual earthquake is a result of strain release during the elastic rebound.



Observed displacements due to San Francisco earthquake (a) and process of strain accumulation in the vicinity of a fault (b).



Principal of survey results.

¹³ Reid, H.F. 1910. The Mechanics of the Earthquake. In 'The California Earthquake of April 18, 1906, Report of the State Investigation Commission'. Vol.2, Washington D.C. Carnegie Institution, pp. 1-192.

HASKELL

When considering a seismic source as a constantly moving dislocation of adjacent blocks and assuming

1. constant rupture velocity ' v_r ' and a
2. rectangular source shape (area = length x width)
3. ramp source time function
4. final displacement

we speak of a 'Haskell' model¹⁴. Assuming ' x ' is orientated parallel to the strike of the fault, the displacement at ' x '

$$u(t) = u_{\infty} G \left(t - \frac{x}{v_r} \right)$$

with ' u_{∞} ' represents the final displacement (=half the fault slip 'D'), and 'G' is the 'ramp function'.

The far-field displacement of this simple line source for P- and S-waves - that is beyond several wave lengths - is trapezoidal shaped (symmetric ramp source time function). The latter is an effect of a convolution of two boxcar functions (s.a. Lay & Wallace, 1995, p.367) which depends on

1. the displacement history of a single particle along the line source (rise time), and
2. the finiteness of the source (rupture duration)

The radial component (P-wave) of the far-field displacement of a double couple source is described by:

$$u_r(r, t) = \frac{1}{4\pi\rho v_P^3} \frac{R_P}{r} \dot{M} \left(t - \frac{r}{v_P} \right)$$

with R_P = radiation pattern of P-wave, ρ = density, v_P = P-wave velocity and \dot{M} = moment rate. Adding up all 'N' subevents at distance ' r_i ' and considering their time-lags ' Δt_i ' leads to

$$u(r, t) = \sum_{i=1}^N u_i \left(r_i, t - \frac{r}{v_P} - \Delta t_i \right)$$

Because, $\dot{M}(t) = GA_i \dot{D}_i(t)$ and $A_i = w dx$, with w = width, we may rewrite the formulae as

$$u_r(r, t) = \frac{R_i^P G}{4\pi\rho v_P^3} w \sum_{i=1}^N \frac{\dot{D}_i}{r_i} (t - \Delta t_i) dx$$

¹⁴ Haskell, N.A. 1964. Total energy and energy spectra density of elastic waves from propagating faults. Bull.Seism.Soc.Am., Vol.54, 1811-1841.

At larger distances perpendicular to the fault ‘ R^P ’ and ‘ r_1 ’ are approximately constant. If a constant rupture velocity ‘ v_r ’ is assumed, the displacement history on the fault is everywhere the same. Then $\Delta t_i = x/v_r$, with ‘ x ’= fault length. Using the shift property we may rewrite the velocity time history as

$$\dot{D}\left(t - \frac{x}{v_r}\right) = \dot{D}(t) * \delta\left(t - \frac{x}{v_r}\right)$$

hence, the particle velocity is everywhere the same. Because the velocity ‘ \dot{D} ’ is independent of ‘ x ’, it can be taken outside of the integral,

$$u_r(r, t) = \frac{R^P G}{4\pi\rho v_p^3} w \frac{\dot{D}(t)}{r} \int_0^x \delta\left(t - \frac{x}{v_r}\right) dx$$

Integrating the delta (Dirac) function requires substituting ‘ $z = t - (x/v_r)$ ’, ‘ $x = t v_r - z v_r$ ’ and ‘ $dx = (dx/dz)dz = -v_r dz$ ’ and considering the identity

$$\int_0^x \delta\left(t - \frac{x}{v_r}\right) dx = \int_t^{t - \frac{x}{v_r}} -v_r \delta(z) dz$$

The integral of $\delta(z)$ is the Heaviside step function ‘ $H(t)$ ’ which is ‘0’ before the arrival ‘ $t = x/v_r$ ’ of the wave and ‘1’ for ‘ $t > 0$ ’.

$$u_r(r, t) = \frac{R^P G w}{4\pi\rho v_p^3} \frac{\dot{D}(t)}{r} * v_r H(z) \quad \left|_{t - \frac{x}{v_r}}^t = \frac{R^P G w v_r \dot{D}(t)}{4\pi\rho v_p^3 r} * \left[H(t) - H\left(t - \frac{x}{v_r}\right) \right] \Rightarrow \right.$$

$$u_r(r, t) = \frac{R^P G w v_r \dot{D}(t)}{4\pi\rho v_p^3 r} * B(t, x/v_r)$$

with ‘ B ’ being a boxcar of duration ‘ x/v_r ’. Calculating the ‘area’ under the far-field P-wave pulse for arriving at the seismic moment, we have to integrate over the time:

$$\int_{-\infty}^{\infty} u_r(r, t) dt = \int_{-\infty}^{\infty} \frac{R^P G w v_r \dot{D}(t)}{4\pi\rho v_p^3 r} * B(t, x/v_r) dt \Rightarrow$$

$$r \frac{4\pi\rho v_p^3}{R^P} \int_{-\infty}^{\infty} u_r(r, t) dt = \int_{-\infty}^{\infty} G w v_r B(t, x/v_r) * \dot{D}(t) dt$$

The left-hand side is the area under the displacement pulse corrected for spreading, radiation pattern and material constants. The right-hand side equals the seismic moment (GAD), with G = shear modulus, $A = wl = wv_r B(t, x/v_r)$, and D = the integral of $\dot{D}(t)$ over time. Note, that the convolution of ‘ B ’ and ‘ $\dot{D}(t)$ ’ result in a trapezoid signal in the far-field.

BRUNE

General:

The model of Brune¹⁵ considers simultaneous slip along the fault (x-axis), that initiates a shear wave propagating perpendicular to the fault surface (y-axis). It is assumed, that a tangential stress step is applied to the interior of a fault plane, causing both sides of the blocks to move in opposite directions.

The shear stress in excess of the dynamic friction shear stress at a point along the 'y-axis' is

$$\sigma(y, t) = \sigma_{eff} H(t - y/v_S)$$

where 'H(t)' is the Heaviside function, 'v_S' = shear wave velocity, and 'σ_{eff}' is the effective shear stress (actual shear stress minus dynamic shear stress level due to friction). Because

$$\begin{aligned} G \left(\frac{\partial u}{\partial y} \right) &= -\sigma(y, t) \\ \dot{u}(t) &= \left(\frac{\sigma_{eff}}{G} \right) v_S H(t - y/v_S) \\ &\text{and for } t \geq y/v_S \Rightarrow \\ u(t) &= \left(\frac{\sigma_{eff}}{G} \right) v_S (t - y/v_S) \end{aligned}$$

Along the fault ('y' = 0, and 't' small), the displacement increases linearly (du/dt = constant) in time.

$$\begin{aligned} u(t) &= \left(\frac{\sigma_{eff}}{G} \right) v_S t \\ \dot{u}(t) &= \left(\frac{\sigma_{eff}}{G} \right) v_S \end{aligned}$$

The spectrum of the displacement observed along the fault is therefore

$$\Omega(\omega) = \int_0^\infty \left(\frac{\sigma_{eff}}{G} \right) v_S t e^{-\omega t} dt = -\frac{1}{\omega^2} \frac{\sigma_{eff} v_S}{G}$$

15 Brune, J. 1970, 1971. Tectonic stress and the spectra of seismic shear waves from earthquakes. J.Geophys.Res. 75, 1970, 4997-5009 (correction in J.Geophys.Res. 76, 1971, 5002).

Brune's approach:

Once the effects of the edges of the fault plane are recognized at the point of observation, the particle velocity will decrease and approach zero at times larger compared to the distance 'r' to edge divided by the shear velocity. Therefore, Brune introduced a time constant equivalent to the travel time of the shear wave $\tau = r/v_s$, so that

$$u(y = 0, t) = \left(\frac{\sigma_{eff}}{G} \right) v_s \tau (1 - e^{-t/\tau}) \quad \text{and}$$
$$\dot{u}(y = 0, t) = \left(\frac{\sigma_{eff}}{G} \right) v_s e^{-t/\tau}$$

This change takes care of the near-field effect of the finite dislocation size. The corresponding Fourier transform yields

$$\Omega(\omega) = \frac{\sigma_{eff} v_s}{G} \frac{1}{\omega} \sqrt{\frac{1}{\omega^2 + \frac{1}{\tau^2}}} = \frac{\sigma_{eff} v_s}{G} \frac{1}{\omega} \sqrt{\frac{1}{\omega^2 + \omega_c^2}}$$

where ' $\omega_c = 1/\tau = 2\pi f_c$ ', with ' f_c ' as the corner frequency of the displacement spectrum.

Further conclusions were drawn by Brune when he considered Keilis-Borok's work (1959)¹⁶. Thus, the seismic moment ' M_0 ' is related to the third power of the source radius 'r':

$$M_0 = G A \bar{D}$$
$$A = r^2 \pi$$
$$\bar{D} = \frac{2}{3} D_{max} = \frac{\sigma_{eff}}{G} r \frac{16}{7\pi}$$
$$M_0 = \sigma_{eff} r^3 \frac{16}{7}$$

if the drop of the effective shear stress is 100%. The source radius can be estimated from the spectrum via the corner frequency ' f_c ' (of the shear wave propagating with ' v_s ')

$$r = \frac{2.34 v_s}{\omega_c} = \frac{2.34 v_s}{2\pi f_c}$$

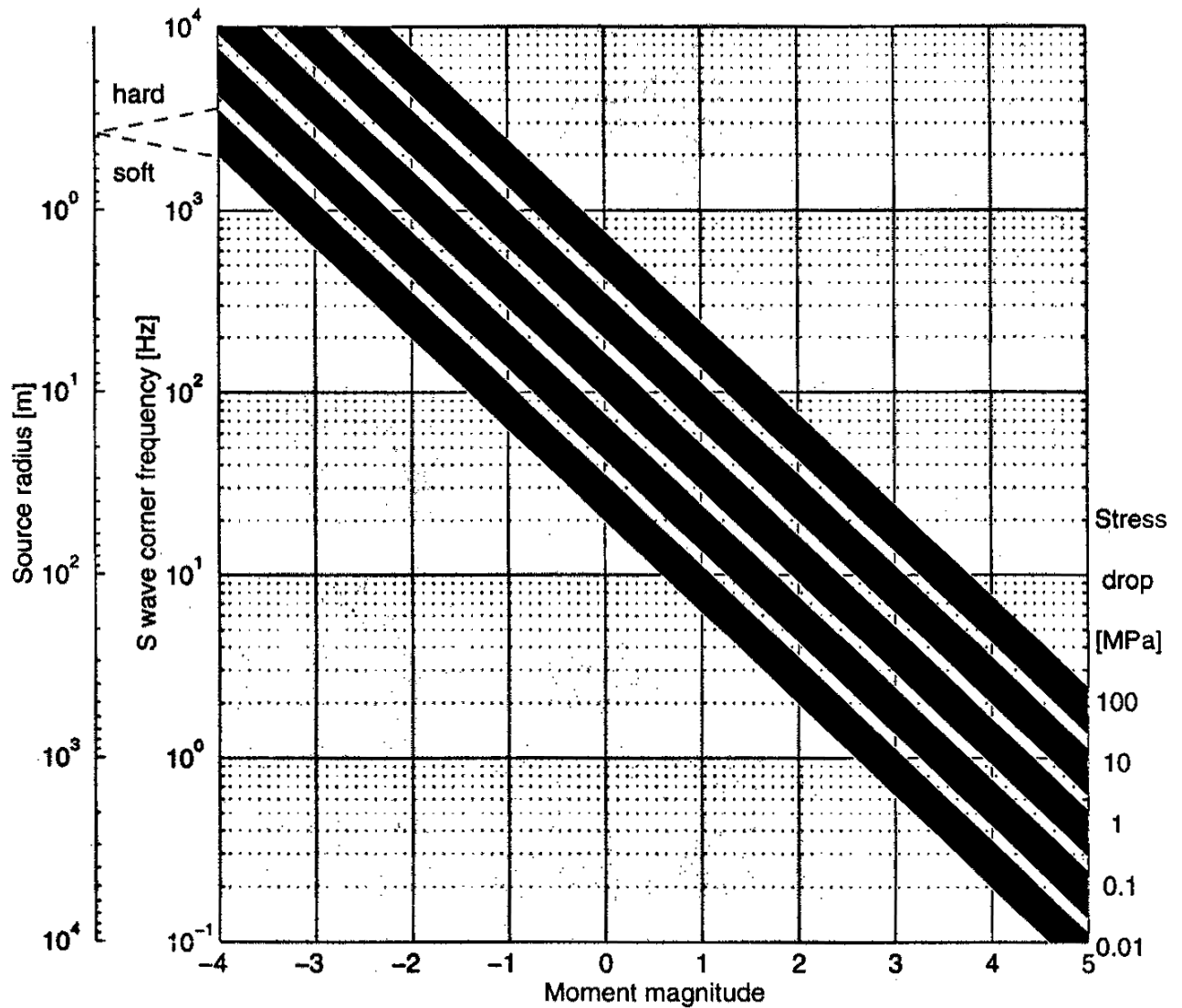
Note, that the constant factor '2.34' applies only to a circular source, which can be described by the radius 'r'.

¹⁶ Keilis-Borok, V.I. 1959. On estimation of the displacement in an earthquake source and of source dimensions. Ann. Geofis. 12, 205-214.

Considering the following parameters

	Density ρ (kg/m ³)	Shear modulus G (GPa)	Shear wave velocity v_s (m/s)
Hard rock	2700	37	3700
Soft rock	1800	7.2	2000

Mendecki (1997)¹⁷ summarized the most important parameters of the Brune's model:

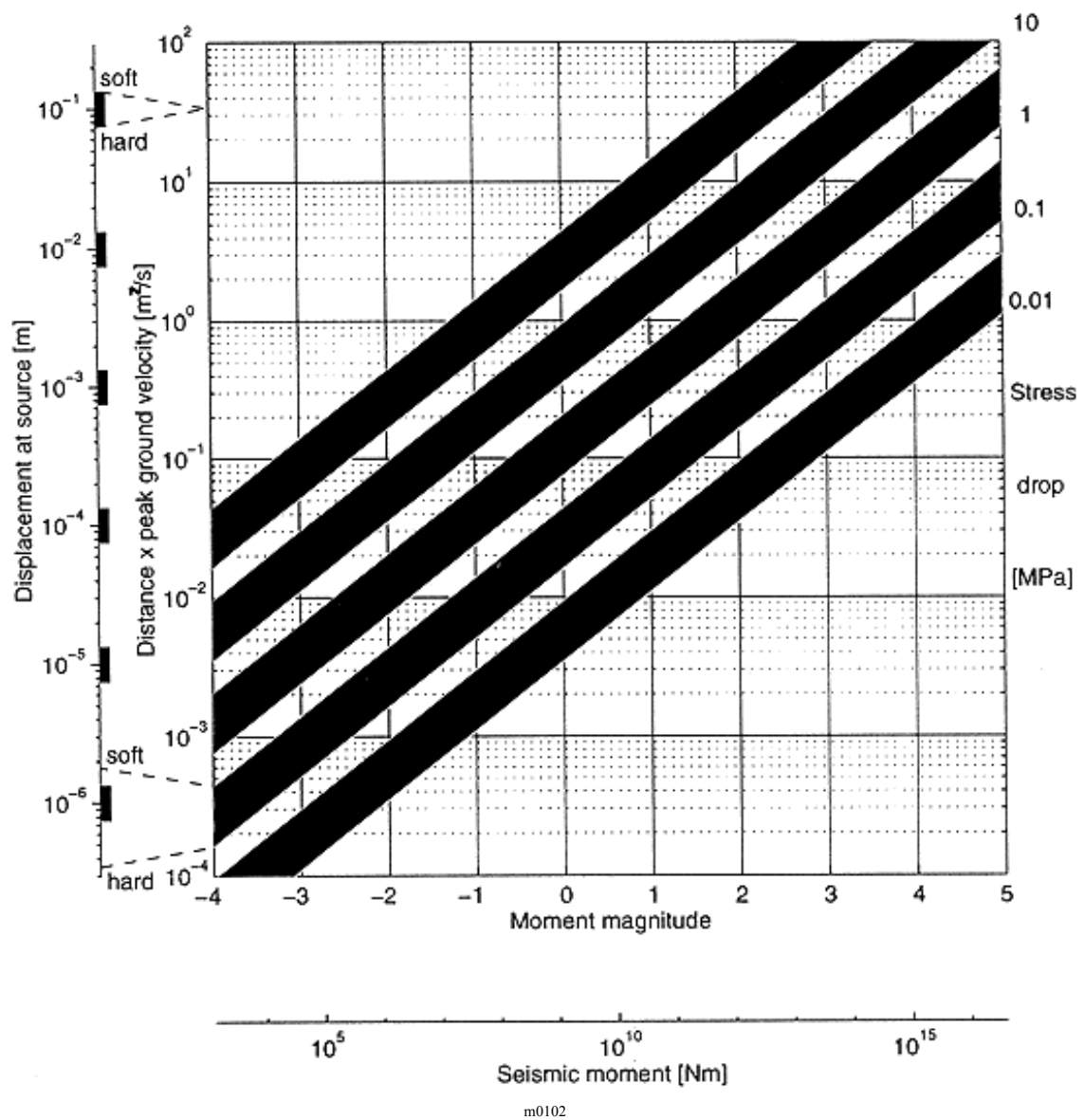


m0101

Note, that the moment magnitude is estimated from Hanks & Kanamori's ' $M_w = 0.67 \log(M_0) - 6.1$ ', thus it is independent of the shear stress drop in the diagram shown above.

¹⁷ Mendecki, A.J. 1997. Seismic Monitoring in Mines. Chapman & Hall.

The picture below illustrates source displacements and far field peak velocities, is also taken from Mendecki (1997)¹⁸. Note again, that the moment magnitude is estimated from Hanks & Kanamori's ' $M_W = 0.67 \log(M_0) - 6.1$ ', thus it is independent of the shear stress drop in the diagram shown below.



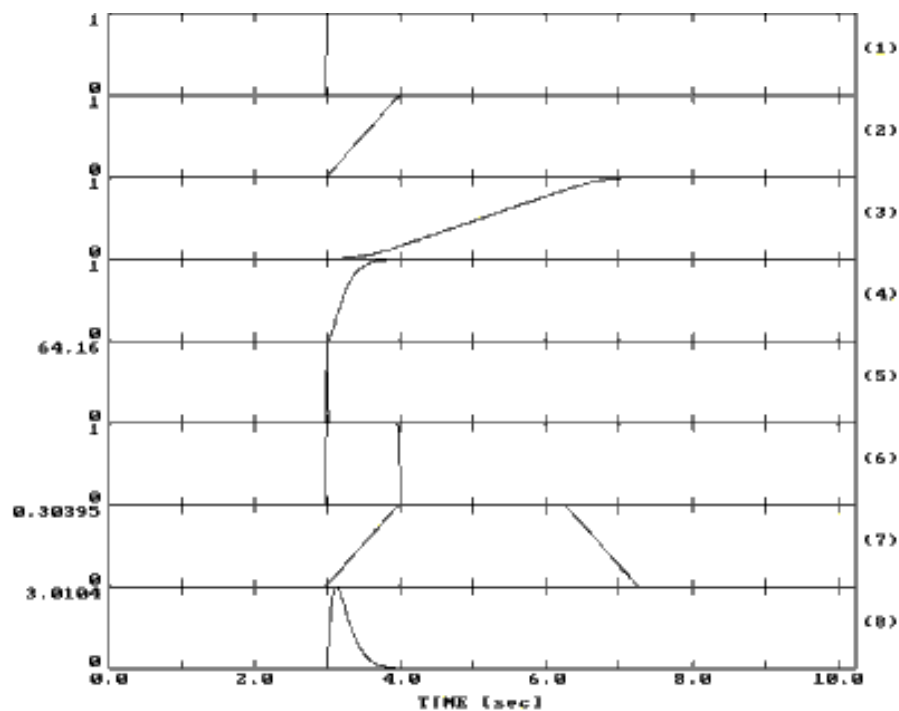
¹⁸ Mendecki, A.J. 1997. *Seismic Monitoring in Mines*. Chapman & Hall.

COMPARISON OF MODELS

All three models differ in their source time function. The top four traces show the respective displacement functions

1. instant displacement regardless of rupture length ('Reid')
2. linear growing displacement
3. smoothly growing displacement ('Haskell')
4. displacement starting suddenly and slowing down ('Brune')

The bottom four traces show the respective time-derivatives of the source time functions, as if the displacement would be recorded in the far field (equivalent to the derivative of the seismic moment).



Note, that the spectra decay differently, depending on the type of the source time function and their respective time-derivative:

Spectrum of time-derivatives:

Type

1. does not decay at all
2. first no decay, then decays with ω above the corner frequency
3. first no decay, then decays with ω^2 above the corner frequency
4. first no decay, then decays with ω and finally with ω^2

SOURCES OF ERRORS

LOCATION

Due to local travel time delays or wrong onset pickings, the location of seismic events can be severely hampered. Wrong locations lead to wrong magnitudes, moment tensors, fault plane solutions, etc.

As an example see also Wong, I.G. & McGarr, A. 1990. Implosional failure in mining-induced seismicity: A critical review. 2nd Int. Symposium on 'Rockburst and Seismicity in Mines', Balkema, 45-52.

BANDWIDTH

If the frequency content of seismic signals exceeds the bandwidth of the recordings, serious underestimations of the seismic moment occur. Consequently, moment tensor inversions lead to wrong mechanisms.

See Di Bona, M. & Rovelli, A. 1988. Effects of the bandwidth limitation on stress drops estimated from integrals of the ground motion. Bull.Seism.Soc.Am., Vol.78, 1818 -1825.

FOCAL SPHERE COVERAGE

The focal sphere is usually not equally covered with stations thus the statistical significance of focal solutions is a) different for each event and b) often insufficient.

WAVEFORM MODELLING

Empirical Green Functions are subject to local variations and may lead to wrong moment tensors.

STATION CORRECTIONS

Time delays and waveform distortions due to absorption may result in wrong locations and wrong energy estimates, thus resulting in wrong magnitudes...

INVERSION OF SCALING LAWS

Generally speaking, scaling laws should not be 'inverted'. The constants in $Y = a + b \cdot X$ are usually not comparable with $X = c + d \cdot Y$ with $c = -a/b$ and $d = 1/b$.

As an example see also Wells, D.L. & Coppersmith, K.J. 1994. New empirical relationships among magnitude, rupture length, rupture width, rupture area and surface displacement. Bull.Seism.Soc.Am., Vol.84, No.4, 974-1002.